

PAPER • OPEN ACCESS

# Xeno-free bioengineered human skeletal muscle tissue using human platelet lysate-based hydrogels

To cite this article: Xiomara Fernández-Garibay *et al* 2022 *Biofabrication* 14 045015

View the [article online](#) for updates and enhancements.

## You may also like

- [Absolute quantification of carnosine in human calf muscle by proton magnetic resonance spectroscopy](#)  
Mahir S Özdemir, Harmen Reyngoudt, Yves De Deene *et al.*
- [Multiscale engineered human skeletal muscles with perfusable vasculature and microvascular network recapitulating the fluid compartments](#)  
Hyeonyu Kim, Tatsuya Osaki, Roger D Kamm *et al.*
- [3D-bioengineered model of human skeletal muscle tissue with phenotypic features of aging for drug testing purposes](#)  
Rafael Mestre, Nerea García, Tania Patiño *et al.*



## Breath Biopsy<sup>®</sup> OMNI

The most advanced, complete solution for global breath biomarker analysis

SEE WHAT OMNI  
CAN DO FOR YOU



# Biofabrication



## PAPER

### OPEN ACCESS

RECEIVED  
23 May 2022

REVISED  
5 August 2022

ACCEPTED FOR PUBLICATION  
30 August 2022

PUBLISHED  
13 September 2022

Original content from this work may be used under the terms of the [Creative Commons Attribution 4.0 licence](https://creativecommons.org/licenses/by/4.0/).

Any further distribution of this work must maintain attribution to the author(s) and the title of the work, journal citation and DOI.



# Xeno-free bioengineered human skeletal muscle tissue using human platelet lysate-based hydrogels

Xiomara Fernández-Garibay<sup>1</sup> , Manuel Gómez-Florit<sup>2,3</sup> , Rui M A Domingues<sup>2,3</sup> ,  
Manuela E Gomes<sup>2,3</sup> , Juan M Fernández-Costa<sup>1,\*</sup> and Javier Ramón-Azcón<sup>1,4,\*</sup>

<sup>1</sup> Institute for Bioengineering of Catalonia (IBEC), The Barcelona Institute of Science and Technology (BIST), Baldiri Reixac 10-12, 08028 Barcelona, Spain

<sup>2</sup> 3B's Research Group, I3Bs-Research Institute on Biomaterials, Biodegradables and Biomimetics, University of Minho, Avepark, Zona Industrial da Gandra, 4805-017 Barco-Guimarães, Portugal

<sup>3</sup> ICVS/3B's—PT Government Associate Laboratory, Braga/Guimarães, Portugal

<sup>4</sup> Institució Catalana de Reserca i Estudis Avançats (ICREA), Passeig de Lluís, Companys, 23, 08010 Barcelona, Spain

\* Authors to whom any correspondence should be addressed.

E-mail: [jfernandez@ibecbarcelona.eu](mailto:jfernandez@ibecbarcelona.eu) and [jramon@ibecbarcelona.eu](mailto:jramon@ibecbarcelona.eu)

**Keywords:** skeletal muscle, tissue engineering, xeno-free, 3D culture, platelet lysate

Supplementary material for this article is available [online](#)

## Abstract

Bioengineered human skeletal muscle tissues have emerged in the last years as new *in vitro* systems for disease modeling. These bioartificial muscles are classically fabricated by encapsulating human myogenic precursor cells in a hydrogel scaffold that resembles the extracellular matrix. However, most of these hydrogels are derived from xenogenic sources, and the culture media is supplemented with animal serum, which could interfere in drug testing assays. On the contrary, xeno-free biomaterials and culture conditions in tissue engineering offer increased relevance for developing human disease models. In this work, we used human platelet lysate (PL)-based nanocomposite hydrogels (HUgel) as scaffolds for human skeletal muscle tissue engineering. These hydrogels consist of human PL reinforced with aldehyde-cellulose nanocrystals (a-CNC) that allow tunable mechanical, structural, and biochemical properties for the 3D culture of stem cells. Here, we developed hydrogel casting platforms to encapsulate human muscle satellite stem cells in HUgel. The a-CNC content was modulated to enhance matrix remodeling, uniaxial tension, and self-organization of the cells, resulting in the formation of highly aligned, long myotubes expressing sarcomeric proteins. Moreover, the bioengineered human muscles were subjected to electrical stimulation, and the exerted contractile forces were measured in a non-invasive manner. Overall, our results demonstrated that the bioengineered human skeletal muscles could be built in xeno-free cell culture platforms to assess tissue functionality, which is promising for drug development applications.

## 1. Introduction

Engineered human skeletal muscle tissues are promising new tools to accelerate the drug development process of muscle-related diseases, such as muscular dystrophies. In particular, these engineered tissues represent more efficient and predictive *in vitro* models that can be used in preclinical research stages, complementing traditional 2D assays and reducing the need for animal models [1, 2]. Advances generated in this field could also be applied to regenerative medicine. Concretely, tissue replacements could be

engineered at a larger scale to treat volumetric muscle loss [3, 4]. Native skeletal muscle tissue comprises aligned multinucleated fibers formed by the fusion and differentiation of muscle precursor cells [5, 6]. Therefore, tissue engineering strategies are based on encapsulating muscle precursor cells in a suitable biomaterial scaffold that mimics the extracellular matrix (ECM) 3D architecture and provides topographical and microenvironmental cues to guide cell alignment and fusion [2].

Nowadays, the most common biomaterials used for skeletal muscle tissue engineering are gelatin

methacryloyl (GelMA) [7–13], collagen [3, 14–16], and fibrin [17–27]. These natural biomaterials are usually modified or reinforced to improve their mechanical or biological properties. For instance, photocrosslinkable GelMA has been combined with other biomaterials such as cellulose, alginate, or poly(ethylene glycol) (PEG), to generate long-lasting micropatterned composite hydrogels with a slower degradation rate [11–13]. On the other hand, collagen and fibrin have been widely combined with Matrigel® [16, 20, 22, 25–27] or Geltrex™ [19, 24] to enhance their structural properties. Matrigel® and Geltrex™ are commercial basement membrane ECM products derived from the Engelbreth–Holm–Swarm (EHS) murine tumor cells. These biomaterials contain various structural proteins, including laminin, collagens (mainly collagen IV), entactin, and the heparin sulfate proteoglycan perlecan [28]. Moreover, these EHS matrices have several tumor-derived growth factors, cytokines, and enzymes contributing to their biological function [29, 30]. Although these have been valuable materials for 3D cell culture, their complex, ill-defined, and highly variable batch-to-batch composition compromises the reproducibility and accuracy of cell-based assays [29, 31, 32]. Furthermore, these materials are not xeno-free. Nearly all 3D models of human skeletal muscle published to date have used materials derived from xenogenic tissues, such as gelatin from porcine skin [10, 13, 17], collagen from rat tail [10, 16], fibrinogen from bovine plasma [19, 24–27], or decellularized ECM from porcine muscle [33]. This limits any clinical application of engineered tissues in regenerative medicine due to the possible presence of xenogenic contaminants from animal-derived ECM [34, 35]. Moreover, animal-derived serum in culture media could reduce sensitivity to drug toxicity within *in vitro* testing platforms [36].

Platelet lysate (PL) from human plasma is an attractive alternative biomaterial for xeno-free scaffold formation. PL formulations are prepared by pooling platelet concentrates from several donors and freeze/thaw cycles that cause platelet disruption without adding any clot activator to release PL content, resulting in a reproducible batch-to-batch composition [37–39]. Apart from a rich environment of growth factors and cytokines, PL contains ECM precursors like fibrinogen and vitronectin. Hence, PL hydrogels can be formed through thrombin-activated induction of the coagulation cascade, obtaining fibrin-based fibrillar gels [40]. Although these are exciting materials, their potential as scaffolds for 3D cell culture is restricted by their poor structural stability and mechanical properties [41]. Additionally, the intrinsic PL growth factors and cytokines are not well-retained in PL gels [40]. To overcome these limitations, PL gels can be reinforced with nanomaterials that provide additional functionalities.

Mendes *et al*, have developed a nanocomposite fibrillar hydrogel (HUGel) based on the induction of the human PL coagulation cascade while incorporating cellulose nanocrystals (CNC) modified with surface aldehyde groups aldehyde-cellulose nanocrystals (a-CNC) [42]. In this material, the a-CNC act both as nanofillers entrapped in the PL fibril structure, and crosslinkers through reversible Schiff base bonds with the amine groups of the PL proteins. The resulting nanocomposite hydrogels have tunable mechanical and biochemical properties that can modulate the behavior of encapsulated stem cells, such as human adipose-derived stem cells (hASCs). It has been demonstrated that increasing a-CNC content in PL hydrogels causes an increase in fiber diameter, interfibrillar porosity, and stiffness. Moreover, a-CNC loading hinders the typical fast clot retraction and improves bioactive molecule retention, controlling the 3D cell microenvironment. HUGel has also been used as bioink for bioprinting hierarchical fibrillar structures for stem cell 3D cell culture without the need for animal-derived serum supplementation [43]. For instance, the serum-free cell culture of hASCs in HUGel was compared to those in GelMA and alginate bioinks. The results showed that, in contrast to the other polymers, HUGel enhances cell spreading and proliferation, and stimulates the production of cell-secreted ECM.

Here, we employed this human PL-based nanocomposite hydrogel as a scaffold for the 3D culture of human muscle satellite stem cells. This xeno-free model was developed by encapsulating human muscle satellite stem cells in HUGel around a pair of flexible posts in hydrogel casting platforms. The a-CNC content was modulated to favor uniaxial tension, self-organization, cell fusion, and differentiation into long multinucleated myotubes. Furthermore, the functionality of the bioengineered human skeletal muscle tissues was demonstrated by force measurements of the electrical stimulation-induced contractions. Overall, these results show the great potential of human PL-based nanocomposite hydrogels for *in vitro* models of skeletal muscle tissue. These bioengineered human tissues could be used as models for muscular diseases by incorporating patient-derived PL and satellite cells. Remarkably, the xeno-free characteristics of this *in vitro* 3D model could enable the transition into clinical applications for regenerative medicine.

## 2. Experimental procedure

### 2.1. Cell culture

Human immortalized muscle satellite stem cells (HuMSCs) [44] were provided by Dr Bénédicte Chazaud from the Institut NeuroMyoGène, Lyon, France. Primary muscle satellite stem cells were previously isolated from a healthy 14 year-old muscle

biopsy and immortalized using CDK-4/hTERT expression. Cells expressing PAX7 were grown in Skeletal Muscle Basal Medium (PromoCell), containing skeletal muscle supplemental mix (#C-39365, PromoCell), 1% v/v penicillin/streptomycin (P/S, 10 000 U ml<sup>-1</sup>, Thermo Fisher Scientific), and 10% v/v fetal bovine serum (FBS, Thermo Fisher Scientific). The growth medium added after cell encapsulation did not contain FBS but was supplemented with 1 mg ml<sup>-1</sup> of 6-amino-n-caproic acid (ACA, Sigma-Aldrich). The differentiation medium (DM) consisted of Dulbecco's modified eagle medium (DMEM), high glucose, GlutaMAX™ (Gibco, Thermo Fisher Scientific), 1% v/v Penicillin-Streptomycin-Glutamine (P/S-G, 100 X, Gibco, Thermo Fisher Scientific), 1% v/v Insulin-Transferrin-Selenium-Ethanolamine supplement (ITS-X, 100 X, Gibco, Thermo Fisher Scientific), and 1 mg ml<sup>-1</sup> of ACA.

## 2.2. Fabrication of the hydrogel casting platforms

The hydrogel casting platforms were designed using Fusion 360 software (Autodesk) as circular chips (8 mm diameter) with a rectangular well of 35  $\mu$ l volumetric capacity, containing two T-shaped posts (diameter: 0.8 mm; height: 3.25 mm) (figure S1(a)). In this protocol, polydimethylsiloxane (PDMS) replicas of a 3D printed master mold were obtained by Ecoflex™ (00-30, Smooth-On) negative intermediary molds (figure S1(c)) [45].

### 2.2.1. Fabrication of the master molds

First, the master mold was generated by transforming the platform design into an standard triangle language (STL) file for projector-based stereolithography 3D printing using a Solus digital light processing (DLP) 3D Printer (Reify 3D) with an opaque orange resin (SolusProto, Reify 3D) that withstands high temperatures. The hard 3D printed molds were silanized by chemical vapor deposition of trichloro(1H,1H,2H,2H-perfluorooctyl)silane (PFOTS, Sigma-Aldrich). Briefly, the surface of 3D printed molds was activated with oxygen plasma for 30 s and immediately placed in a vacuum desiccator with five drops of PFOTS for 1 h. After deposition, the silanized 3D printed master mold was left in an oven for 1 h at 80 °C.

### 2.2.2. Fabrication of the negative molds

The Ecoflex™ negative mold was made by mixing the two prepolymers (1A:1B, approximately 15 g of each prepolymer). Before beginning, prepolymer B had to be thoroughly pre-mixed. Then, A and B were thoroughly mixed for 3 min. The mixture was placed in a vacuum desiccator for 5 min to remove entrapped air. After, the liquid prepolymer was poured on the 3D printed master mold and degassed inside the vacuum desiccator for 15 min. The Ecoflex™ was cured at room temperature overnight. Finally, the

cured polymer was carefully peeled off from the 3D printed master mold, washed with ethanol, and dried with N<sub>2</sub> flow and on a hot plate (90 °C, 10 min) before silanization with PFOTS (following the same procedure as with the 3D printed master mold).

### 2.2.3. Replica molding of PDMS platforms

The PDMS polymer elastomer base and curing agent were weighted in a 10:1 ratio. After thoroughly mixing, we degassed the polymer in a vacuum desiccator. The uncured PDMS was poured on the Ecoflex™ mold (placed in a glass Petri dish), and the trapped air in the post area was removed with a syringe. Then, the mold was left inside a vacuum desiccator until all the trapped air was removed. After, the PDMS was cured at 80 °C for 6 h. Before demolding, PDMS was left for additional curing at room temperature overnight. PDMS was then detached from the Ecoflex™ and cleaned by sonication in Milli-Q water and 2-propanol for 5 min. Then, individual PDMS platforms were cut using an 8 mm diameter biopsy punch. Finally, a cover glass was bonded to each platform base by activating the glass and PDMS platform base with ultraviolet (UV) plasma for 15 min before joining the two surfaces. Before cell encapsulation, platforms were washed with 2-propanol and water.

## 2.3. Preparation of the nanocomposite hydrogel (HUGel)

### 2.3.1. Preparation of HUGel precursors

Human PL was purchased from STEMCELL™ Technologies. a-CNC were prepared at the Research Institute on Biomaterials, Biodegradables, and Biomimetics (I3Bs, University of Minho, Portugal). CNC were extracted from microcrystalline cellulose powder (Sigma-Aldrich) by sulphuric acid hydrolysis. Briefly, concentrated sulphuric acid (Sigma-Aldrich) was added dropwise to the microcrystalline cellulose powder up to a final concentration of 64% w/v. The obtained suspension was heated at 44 °C for 2 h. Then, the suspension was collected and stored at 4 °C. To produce a-CNC, sodium periodate (NaIO<sub>4</sub>, Sigma-Aldrich) was added to a 1.5% w/v CNC aqueous suspension in a 1:1 molar ratio (NaIO<sub>4</sub>:CNC) for 12 h. Finally, the concentration of the working suspension was adjusted by concentrating it against PEG (20.000 kDa, Sigma-Aldrich) using benzoylated cellulose dialysis membranes (2000 Da nominal molecular weight cutoff (NMWCO), Sigma-Aldrich). Stock water dispersions of a-CNC were prepared and fully characterized in our previous works [42, 43].

### 2.3.2. Cell encapsulation by HUGel casting in PDMS platforms

PDMS casting platforms were treated with 0.2% Pluronic® (F-127, Sigma-Aldrich) for 20 min to avoid hydrogel attachment to the PDMS well. After treatment, the platforms were washed three times with

phosphate buffered saline (PBS) and sterilized with UV light. For cell encapsulation, HuMSCs were trypsinized and resuspended in PL. In these experiments, we worked with final cell densities of 0.5, 1, or  $2.5 \times 10^7$  cells  $\text{ml}^{-1}$ . The a-CNC water dispersion was placed in a sterile Eppendorf tube at the desired concentration and sonicated for 5 min. Then, the suspension was mixed with thrombin from human plasma ( $2 \text{ U ml}^{-1}$ , Sigma-Aldrich) and  $\text{CaCl}_2$  (10 mM, Sigma-Aldrich). The cell suspension in PL was thoroughly mixed in a 1:1 ratio with the suspension containing a-CNC, thrombin, and  $\text{CaCl}_2$ . Finally, a volume of  $35 \mu\text{l}$  of the mixture was carefully placed inside each PDMS platform well. The samples were allowed to crosslink at  $37^\circ\text{C}$  for 30 min before adding growth medium (day  $-2$ ). After two days (day 0), the medium was switched to differentiation medium (figure 1(a)). Then, half of the medium was replaced every two days. The 3D culture was carried out under shaking conditions inside an incubator ( $37^\circ\text{C}$ , 5%  $\text{CO}_2$ ).

### 2.3.3. Immunofluorescence staining

The bioengineered human muscle tissues were fixed with 10% formalin solution (Sigma-Aldrich) for 30 min at room temperature (RT), followed by several washes in PBS. Samples were then permeabilized with PBS-T (0.1% Triton-X (Sigma-Aldrich) in PBS) for 15 min at RT, blocked (0.3% Triton-X, 3% donkey serum (Sigma-Aldrich) in PBS) for 2 h at RT, and incubated with monoclonal mouse anti-sarcomeric  $\alpha$ -actinin (SAA) primary antibody (1:200, Sigma-Aldrich) at  $4^\circ\text{C}$  overnight. After several PBS-T washes, the samples were incubated for 2 h with polyclonal donkey anti-mouse IgG, Alexa Fluor 488-conjugated secondary antibody (1:200, Invitrogen), and rhodamine-phalloidin (1:200, Invitrogen) to stain F-actin, at RT. Finally, to detect the nuclei, the samples were counterstained with DAPI (4',6-diamidino-2-phenylindole, Life Technologies). The complete protocol was performed under shaking conditions.

### 2.3.4. Electrical pulse stimulation (EPS)

After 7 d in differentiation medium, the bioengineered 3D human skeletal muscle tissues were subjected to EPS. EPS was performed with a custom-made stimulation plate with graphite electrodes assembled on a 12-well plate lid. First, the stimulation plate containing the tissues was placed inside a Zeiss Axio Observer.Z1/7 microscope outfitted with the XL S1 cell incubator at  $37^\circ\text{C}$  and in a 5%  $\text{CO}_2$  atmosphere. Then, the electrodes were connected to a multifunction generator (NF Corporation), and the frequency and amplitude of the signals were confirmed using a digital oscilloscope (QUIMAT). Finally, the muscle tissues were subjected to a stimulation regime of square pulses with a 10% duty cycle, an electrical field strength of  $1 \text{ V mm}^{-1}$ , and frequencies from

1 to 50 Hz to evaluate tissue response for a total duration of 110 s (figure 4(a)).

### 2.3.5. Imaging

Live-cell imaging was performed with the Zeiss Axio Observer.Z1/7 microscope outfitted with the XL S1 cell incubator. All images were taken at  $37^\circ\text{C}$  and in a 5%  $\text{CO}_2$  atmosphere and processed using the Fiji image processing package, a distribution of ImageJ [46, 47]. In addition, fluorescence images were taken with a ZEISS LSM800 confocal laser scanning microscope and analyzed using the Imaris microscope image analysis software (Oxford instruments).

### 2.3.6. Force measurements

The post deflections during tissue contractions were recorded and analyzed using Fiji. The force-displacement relationship for the posts was estimated using linear bending theory based on previously published protocols [48, 49], by the following formula:

$$F = \frac{6\pi ED^4}{64a^2(3L-a)} \cdot d = k \cdot d.$$

The Young's modulus of the PDMS (E) was previously measured as  $1.6 \pm 0.1 \text{ MPa}$ . Considering the geometry of the posts and dimensions, we calculated a spring constant (k) of  $3.54 \text{ N m}^{-1}$ . The spring constant was used to transform the recorded post deflections (d) into the force generated by the bioengineered 3D skeletal muscle tissues (F) (figure S1(b)).

### 2.3.7. RNA extraction, RT-PCR, and real-time PCR

Total ribonucleic acid (RNA) from xeno-free bioengineered muscles was isolated using the miRNeasy Micro Kit (QIAGEN) following the manufacturer's instructions. cDNA was synthesized using the SuperScript II Reverse Transcriptase kit (Invitrogen), and quantitative polymerase Chain Reaction (PCR) reactions were run using HOT FIREPol® EvaGreen® qPCR Mix Plus (Solis BioDyne) in a Step-One real-time PCR System (Thermofisher). Primer sequences used for gene expression analysis are listed in table S1.

### 2.3.8. Statistical analysis

All group data are expressed as mean  $\pm$  SEM. The comparisons between groups were performed using Prism 8 software (GraphPad) by a two-tailed Student t-test ( $\alpha = 0.05$ ), applying Welch's correction when necessary. Differences between groups were considered significant when  $p < 0.05$ . All experiments were performed with a  $n \geq 3$ .

## 3. Results and discussion

### 3.1. Human skeletal muscle tissue formation in hydrogel casting platforms

Engineered skeletal muscle tissues require specific topographical and microenvironmental signals that

favor cell alignment and fusion into myotubes. When scaffolds are made of compactable biomaterials, such as collagen, EHS matrices, or fibrin, the most common fabrication approach introduces tendon-like attachment points to provide uniaxial tension during ECM remodeling [50]. Following this strategy, fibrin-Matrigel® and fibrin-Geltrex™ hydrogels have been cast in silicone molds with nylon frames or hooks as anchor points [24–27]. The resulting muscle tissue bundles needed to be manipulated and transferred to a different platform for stimulation and force measurements. Another widely used method involves cell-laden matrix compaction around a pair of flexible silicone posts [16, 19, 22–24]. Besides providing uniaxial tension, these hydrogel casting systems allow *in situ* tracking of post deflection due to tissue contraction. Furthermore, these deflections can be transformed into force measurements. Considering these advantages, we fabricated hydrogel casting platforms containing two flexible posts as anchor points (figure S1). The final PDMS platforms were fabricated by replica molding of 3D printed master molds, using Ecoflex™ as reusable intermediary negative molds. Ecoflex™ is a platinum-catalyzed silicone that is cured at room temperature, resulting in a highly stretchable material that can be applied as a fully deformable elastic mold [51]. The individual platforms were designed as circular chips that fit inside 48-well plates. Each platform has a rectangular casting well with a volumetric capacity of 35  $\mu\text{l}$  and contains a pair of posts that direct tissue formation. Crucially, to ensure that tissues are retained under tension, we designed hook-like features on the top of each post.

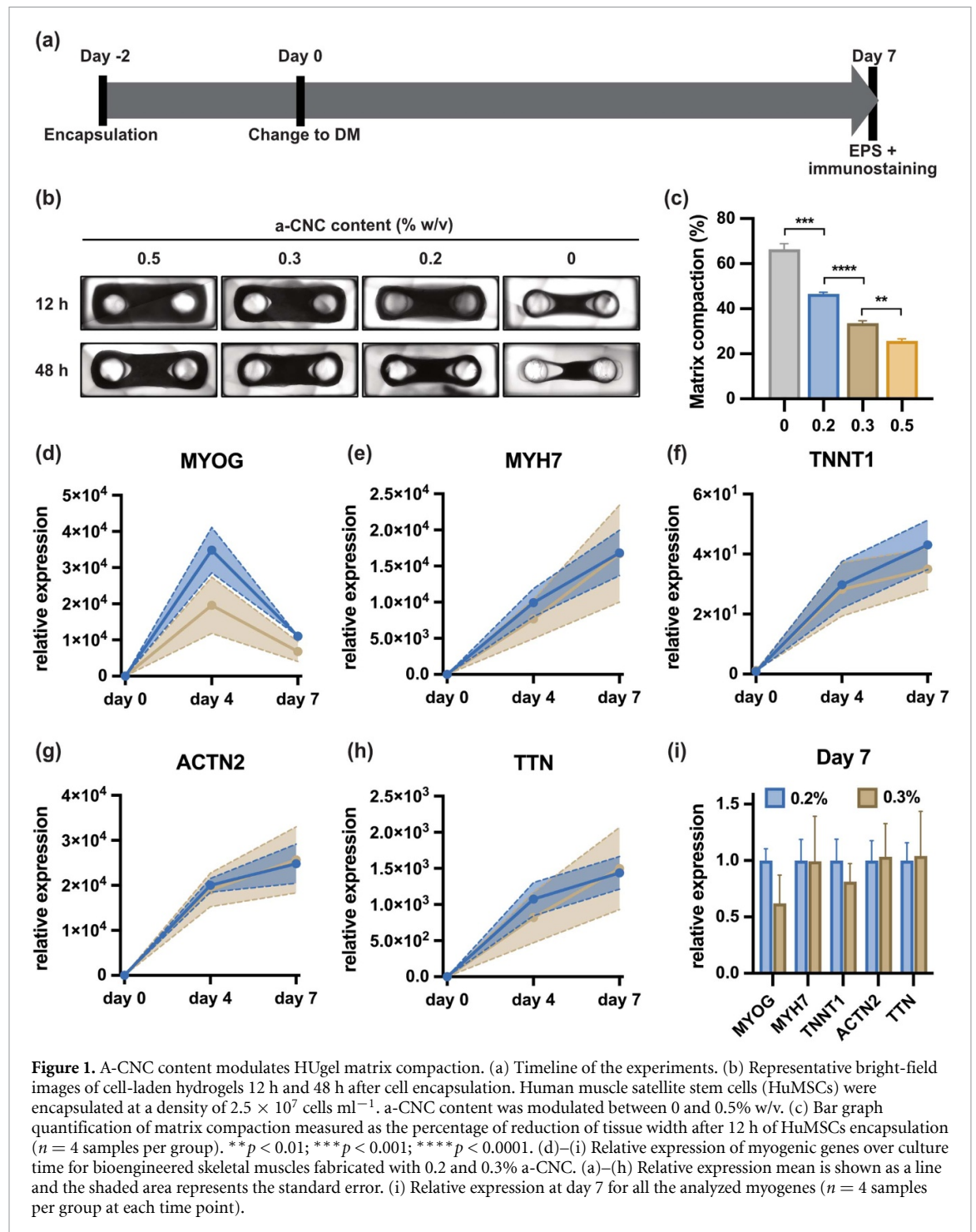
Human PL-based nanocomposite hydrogels (HUGel) were fabricated following a previously published protocol based on the formation of fibrin-based scaffolds [42]. In this work, HuMSCs were encapsulated in HUGel by hydrogel casting in the two-post PDMS platforms. Briefly, a suspension of HuMSCs in PL was mixed with a-CNC water dispersions containing thrombin and calcium ions. We fixed the concentrations of thrombin (1 U  $\text{ml}^{-1}$ ) and  $\text{CaCl}_2$  (5 mM) according to the previous study by Mendes *et al* [42]. For the initial experiments, a-CNC was mixed at a final concentration of 0.5% w/v, and cells were encapsulated at a density of  $5 \times 10^6$  and  $1 \times 10^7$  cells  $\text{ml}^{-1}$ . We observed that the cell-laden HUGel matrix started to detach slowly from the walls of the PDMS well after two days of culture. Hydrogel compaction around the posts due to matrix remodeling by the encapsulated cells could be observed after four days (figure S1(d)). At this time, tissues containing  $1 \times 10^7$  cells  $\text{ml}^{-1}$  were more compacted than those with fewer cells. Matrix remodeling and compaction around the posts is essential in these casting systems to implement uniaxial tension and induce self-organization during tissue formation

[19, 52]. Consequently, cell density was increased to  $2.5 \times 10^7$  cells  $\text{ml}^{-1}$  for future experiments.

### 3.2. a-CNC content can be modulated to promote myotube formation

The physical and biological properties of nanocomposite hydrogels with varying a-CNC content have been extensively characterized in previous studies [42, 43]. Significantly, researchers found that increasing a-CNC content hampers the typical fast densification of the fibrin matrix, which is referred to as clot retraction. In some tissue engineering applications (e.g. for space-filling of wounded tissues), extensive clot retraction is considered an undesirable hydrogel effect. Nevertheless, for skeletal muscle tissue formation, the compaction of the cell-laden matrix around the posts contributes to implementing uniaxial tension that facilitates the self-organization and alignment of myoblasts. At the same time, the matrix remodeling favors myoblast fusion into myotubes. Here, we modified the content of a-CNC to obtain long-lasting scaffolds with high clot retraction properties that promote skeletal muscle tissue formation (figure 1(b)). Encapsulating human skeletal muscle satellite stem cells in a high density of  $2.5 \times 10^7$  cells  $\text{ml}^{-1}$  resulted in HUGel detachment from the wells of the PDMS casting platforms within a few hours of culture. The matrix compaction after 12 h was calculated as the percentage of reduction in tissue width (figure 1(c)). We found that the initial working concentration of 0.5% w/v a-CNC resulted in  $25.7 \pm 1.6\%$  of matrix compaction, whereas the tissues without a-CNC presented extensive compaction of  $66.4 \pm 4.3\%$ . However, the lack of mechanical reinforcement from a-CNC caused hydrogel degradation, so the samples broke and collapsed between 12–60 h after cell encapsulation. On the other hand, hydrogels with a low content of a-CNC (0.3 and 0.2% w/v) offered a high retraction from the beginning of the culture ( $33.6 \pm 2\%$  and  $46.7 \pm 1.1\%$ , respectively) and were stable for at least two weeks.

PL gels are attractive scaffolding materials for stem cell encapsulation because PL contains structural proteins like fibrinogen, as well as growth factors and cytokines that stimulate cell growth and proliferation [38, 41]. However, PL gels alone do not retain these growth factors within the scaffold during culture. Therefore, the impact of a-CNC content on the sequestering and release profile of proteins from the HUGel scaffolds was previously investigated [42]. The results indicated that the a-CNC play an important role in growth factor retention within the HUGel scaffolds due to the formation of a protein corona on the a-CNC surface. This process is mainly driven by the non-covalent protein binding enabled by the nanoparticles surface chemistry [53]. Notably, nanocomposite hydrogels with high a-CNC content (at least 0.61% w/v) are optimal for hASCs



cell encapsulation, where proliferation during cell culture is desired [42, 43]. On the contrary, in skeletal muscle tissue engineering, differentiation of muscle precursor stem cells requires that cells stop proliferating and exit the cell cycle in order to fuse and differentiate into multinucleated myotubes. In fact, all cell culture protocols for differentiating skeletal muscle cells involve removing growth factors and reducing the animal serum present in the basal media [36]. Thus, a microenvironment rich in growth factors could hinder adequate differentiation.

Considering the matrix compaction properties and the expected growth factor release profiles, we selected a-CNC content of 0.2% and 0.3% w/v for the following experiments with HuMSCs. The serum-free growth medium was replaced by serum-free differentiation media 48 h after cell encapsulation (day 0) (figure 1(a)). We analyzed the expression of myogenic genes over culture time and between samples with different a-CNC content (figures 1(d)–(i)). Tissues with 0.2 and 0.3% of a-CNC shared a common profile of myogenic gene expression without any

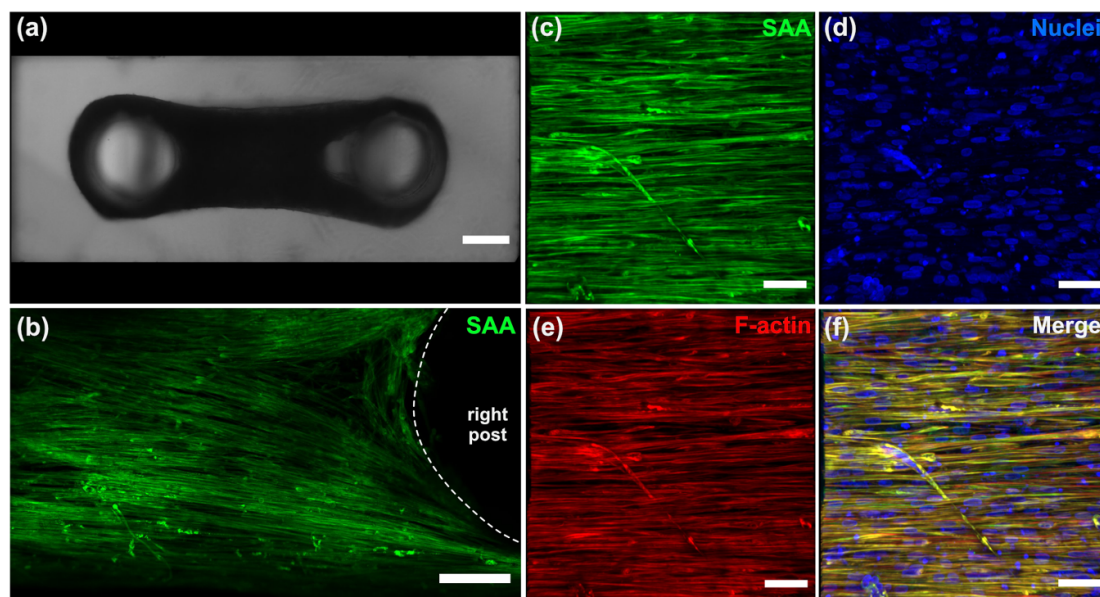


**Figure 2.** Bioengineered *in vitro* 3D human skeletal muscle tissue in a xeno-free culture system. (a) Top-view bright-field image of skeletal muscle tissues in hydrogel casting molds after one week of differentiation. (b)–(f) Representative confocal images showing long, aligned myotubes expressing sarcomeric  $\alpha$ -actinin (SAA, green) in nanocomposite hydrogels containing 0.2% w/v a-CNC. F-actin is stained in red and nuclei in blue. Scale bars: (a) 500  $\mu\text{m}$ , (b) 200  $\mu\text{m}$  (c)–(f) 100  $\mu\text{m}$ .

significant differences. As expected, the expression of myogenin (MYOG), a key developmental regulator for inducing myotube formation [54], was increased after a few days in differentiation conditions (day 4) (figure 1(d)). This increase was followed by a reduction of MYOG expression on day 7, indicating myotube maturation with culture time [55]. Myotube maturation was observed by an increased expression of MYH7 (figure 1(e)), along with the specific striated muscle markers TNN1 (figure 1(f)), ACTN2 (figure 1(g)), and titin (TTN) (figure 1(h)). Furthermore, after seven days in differentiation media, the xeno-free bioengineered muscle tissues were stained for (SAA, green) (figures 2 and S2). The confocal images showed long, highly aligned, multinucleated myotubes expressing SAA.

### 3.3. Nanocomposite hydrogels support the formation of functional human skeletal muscle tissues in a xeno-free cell culture system

The functionality of bioengineered muscle tissues was assessed by their response to EPS. After seven days in differentiation conditions, we performed EPS using graphite electrodes fixed on a modified 12-well plate lid. Following the experiments, immunostaining of electrically stimulated and control (non-stimulated) tissues was carried out (figure 3). Confocal images of SAA stainings showed the presence of striations (white arrows in figure 3(a)), indicating myotube maturation in some of the myotubes. These striated myotubes were only present in electrically stimulated tissues. Nonetheless, we expect that extended culture

periods combined with electrical stimulation training regimes would improve myotube maturation, obtaining uniformly striated myotubes.

As described above, one advantage of hydrogel casting around two flexible posts is performing *in situ* force measurements. In these systems, characterization of the posts' mechanics allows converting the post deflections (caused by contractile tissues) into force measurements [19, 56]. Therefore, measurements are non-invasive and compatible with cell culture conditions.

Bioengineered muscle tissues were subjected to a frequency sweep EPS regime going from low to high frequencies, according to the scheme in figure 4(a). We did not observe any spontaneous contractions without electrical stimulation. However, the electrically stimulated bioengineered human skeletal muscles presented twitch or tetanic contractions depending on the applied frequencies (figures 4(c) and (d)). To compare tissue functionality between different conditions, force measurements were performed for HUgel formulations containing 0.2 (figure 4(e)) and 0.3% w/v a-CNC (figure 4(f)). Notably, increasing a-CNC content led to a significant force reduction, and the maximum tetanus contractile force with 0.3% a-CNC was approximately four times lower than with 0.2% a-CNC (figure 4(g)). Since there were no significant differences in myogenic gene expression between 0.2 and 0.3% a-CNC, other factors might play a more critical role in the measured contractile forces. For instance, the difference in matrix compaction could influence the myotube distribution and



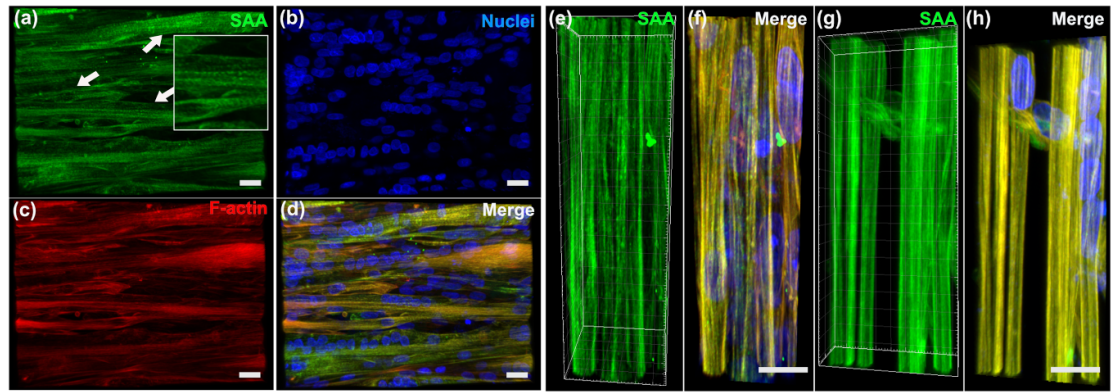


**Figure 3.** Electrically stimulated myotubes present striations after one week of differentiation. (a)–(d) Representative confocal images of electrically stimulated bioengineered human skeletal muscle tissues fabricated with 0.2% w/v a-CNC. White arrows point to striated myotubes. (a) Insert shows zoom-in on the striations. (e)–(h) 3D reconstructions of electrically stimulated myotubes (e), (f) vs myotubes without EPS (g), (h). Striations are only observed in electrically stimulated myotubes. SAA is stained green, F-actin in red, and nuclei in blue. Scale bars: 20  $\mu\text{m}$ .

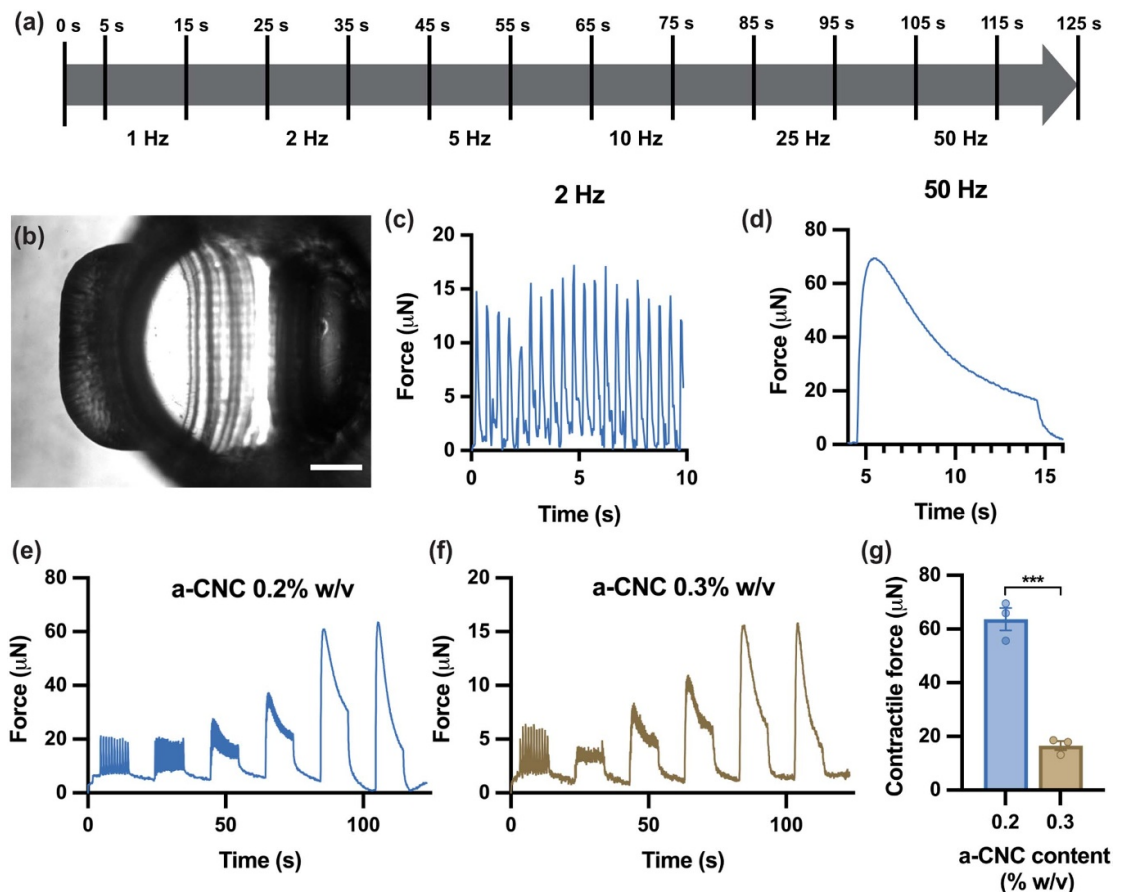


**Figure 4.** Bioengineered 3D human skeletal muscle tissues respond to electrical pulse stimulation (EPS). (a) EPS scheme. (b) Representative top view of a PDMS post used for force measurements. Scale bar: 200  $\mu\text{m}$ . (c), (d) Representative force measurement line graphs obtained for the EPS of tissues containing 0.2% w/v a-CNC show twitch (c) and tetanus (d) contractions with applied frequencies of 2 Hz and 50 Hz, respectively. (e), (f) EPS response from bioengineered human skeletal muscle tissues fabricated with nanocomposite hydrogels containing 0.2% (e) and 0.3% w/v (f) a-CNC. Line graphs represent mean force values ( $n = 3$  samples per group). (g) Bar graph quantification of the maximum tetanus contractile forces generated by the bioengineered human skeletal muscle tissues with 0.3 and 0.2% w/v a-CNC ( $n = 3$  samples per group). \*\*\* $p < 0.001$ .

organization throughout the tissue, and this could result in different force transmission. Furthermore, it has been shown that higher stiffness of engineered muscle tissues can be correlated to lower tetanus

contractile force due to cell-matrix interactions [57]. Given that HUGel formulations with 0.3% a-CNC present a higher theoretical stiffness [42], a stronger response from embedded myotubes could be required

to achieve the same magnitude of post deflection than in formulations with lower a-CNC content.

### 3.4. Perspectives of this work

Altogether, these results highlight the potential of PL-based nanocomposite hydrogels to develop bioengineered skeletal muscle tissues as functional xeno-free *in vitro* models. Taking advantage of the tunable physical and biological properties of these nanocomposite hydrogels, we optimized HUgel's formulation to generate contractile human skeletal muscle tissues. As mentioned above, the maturation of these bioengineered tissues could be enhanced by increasing culture time and electrical stimulation training.

The application of this biomaterial for the 3D cell culture of human adipose stem cells has been explored in previous works [42, 43]. However, at present, HUgel has not been used to generate any tissue models. Furthermore, using this biomaterial would offer several advantages for skeletal muscle tissue engineering, such as the low batch-to-batch variability of its components and its xeno-free characteristics. In fact, there are no xeno-free skeletal muscle tissue models reported to date. For drug development applications, xeno-free tissue models could provide increased relevance by eliminating animal-derived materials and reagents that could reduce sensitivity to drug effects. Additionally, the nature of these nanocomposite hydrogels offers excellent potential to develop personalized tissues from patient-derived PL, which could be used for *in vitro* studies, and at the same time, could have a more straightforward translation from bench to bedside.

## 4. Conclusions

In this work, for the first time, a human PL-based nanocomposite hydrogel (HUgel), consisting of PL and cellulose nanocrystals, was used as a scaffold to develop *in vitro* functional human skeletal muscle tissues in a xeno-free system. The previously reported tunability of the mechanical, biochemical, and structural properties of the HUgel, enabled the generation of long, aligned multinucleated human myotubes in a custom 3D cell culture platform. In addition, this system provided electrical stimulation and supported force measurements of contractile bioengineered human skeletal muscle tissues. Overall, we showed that HUgel has a great potential in skeletal muscle tissue engineering for *in vitro* disease modeling. Remarkably, the xeno-free conditions could also enable future clinical applications in regenerative medicine.

### Data availability statement

All data that support the findings of this study are included within the article (and any supplementary files).


## Acknowledgments

The authors thank the technical support of Micro-FabSpace and Microscopy Characterization Facility, Unit 7 of ICTS 'NANBIOSIS' from CIBER-BBN at IBEC. We would also like to thank the muscle team from the Biosensors for Bioengineering group for their feedback in the review process of this manuscript. Human immortalized muscle satellite stem cells used in this study were kindly provided by Dr Bénédicte Chazaud (Institut NeuroMyoGène (INMG), Lyon, France). This project received financial support from European Research Council program Grant ERC-StG-DAMOC: 714317 (J R-A), European Commission under FET-open program BLOC Project: GA- 863037 (J R-A), Spanish Ministry of Economy and Competitiveness, through the 'Severo Ochoa' Program for Centres of Excellence in R&D: SEV-2016–2019, Spanish Ministry of Economy and Competitiveness: 'Retos de investigación: Proyectos I+D+i': TEC2017-83716-C2-2-R (J R-A), CERCA Programme/Generalitat de Catalunya: 2017-SGR-1079 (J R-A), and Fundación Bancaria 'la Caixa'- Obra Social 'la Caixa': project IBEC-La Caixa Healthy Ageing (J R-A). The authors also acknowledge the European Union's Horizon 2020 research and innovation program under European Research Council Grant Agreement 772817 and Twinning Grant Agreement No. 810850—Achilles. Fundação para a Ciência e a Tecnologia (FCT) for CEECIND/01375/2017 (M G-F) and 2020.03410. CEECIND (R M A D).

## Author contributions

X F-G, J M F-C, M G F, R M A D, and J R-A conceived this work. X F-G and J M F-C performed and coordinated the experiments and data analysis. HUgel material was developed and provided by M G F, M E G, and R M A D. J R-A, M G F, and R M A D acquired the funding for this project. X F-G and J M F-C prepared the manuscript with the supervision of J R-A and input from all the authors.

## ORCID iDs

Xiomara Fernández-Garibay 

<https://orcid.org/0000-0002-0697-985X>

Manuel Gómez-Florit  <https://orcid.org/0000-0001-7758-1251>

Rui M A Domingues  <https://orcid.org/0000-0002-3654-9906>

Manuela E Gomes  <https://orcid.org/0000-0002-2036-6291>

Juan M Fernández-Costa  <https://orcid.org/0000-0002-1854-6082>

Javier Ramón-Azcón  <https://orcid.org/0000-0002-3636-8013>

## References

- [1] Martínez E, St-Pierre J-P and Variola F 2019 Advanced bioengineering technologies for preclinical research *Adv. Phys. X* **4** 1622451
- [2] Fernández-Costa J M, Fernández-Garibay X, Velasco-Mallorquí F and Ramón-Azcón J 2021 Bioengineered *in vitro* skeletal muscles as new tools for muscular dystrophies preclinical studies *J. Tissue Eng.* **12** 204173142098133
- [3] Nakayama K H *et al* 2019 Treatment of volumetric muscle loss in mice using nanofibrillar scaffolds enhances vascular organization and integration *Commun. Biol.* **2** 170
- [4] Moyle L A, Jacques E and Gilbert P M 2020 Engineering the next generation of human skeletal muscle models: from cellular complexity to disease modeling *Curr. Opin. Biomed. Eng.* **16** 9–18
- [5] Chal J and Pourquié O 2017 Making muscle: skeletal myogenesis *in vivo* and *in vitro* *Development* **144** 2104–22
- [6] Mukund K and Subramaniam S 2019 Skeletal muscle: a review of molecular structure and function, in health and disease *Wiley Interdiscip. Rev. Syst. Biol. Med.* **12** e1462
- [7] Shi X, Ostrovidov S, Zhao Y, Liang X, Kasuya M, Kurihara K, Nakajima K, Bae H, Wu H and Khademhosseini A 2015 Microfluidic spinning of cell-responsive grooved microfibers *Adv. Funct. Mater.* **25** 2250–9
- [8] Ebrahimi M, Ostrovidov S, Salehi S, Kim S B, Bae H and Khademhosseini A 2018 Enhanced skeletal muscle formation on microfluidic spun gelatin methacryloyl (GelMA) fibres using surface patterning and agrin treatment *J. Tissue Eng. Regen. Med.* **12** 2151–63
- [9] Costantini M, Testa S, Fornetti E, Barbeta A, Trombetta M, Cannata S M, Gargioli C and Rainer A 2017 Engineering muscle networks in 3D gelatin methacryloyl hydrogels: influence of mechanical stiffness and geometrical confinement *Front. Bioeng. Biotechnol.* **5** 1–8
- [10] Kim W and Kim G 2020 3D bioprinting of functional cell-laden bioinks and its application for cell-alignment and maturation *Appl. Mater. Today* **19** 100588
- [11] García-Lizarribar A, Fernández-Garibay X, Velasco-Mallorquí F, Castaño A G, Samitier J and Ramon-Azcon J 2018 Composite biomaterials as long-lasting scaffolds for 3D bioprinting of highly aligned muscle tissue *Macromol. Biosci.* **18** 1800167
- [12] Ortega M A, Fernández-Garibay X, Castaño A G, De Chiara F, Hernández-Albors A, Balaguer-Trias J and Ramón-Azcón J 2019 Muscle-on-a-chip with an on-site multiplexed biosensing system for *in situ* monitoring of secreted IL-6 and TNF- $\alpha$  *Lab Chip* **19** 2568–80
- [13] Fernández-Garibay X, Ortega M A, Cerro-Herreros E, Comelles J, Martínez E, Artero R, Fernández-Costa J M and Ramón-Azcón J 2021 Bioengineered *in vitro* 3D model of myotonic dystrophy type 1 human skeletal muscle *Biofabrication* **13** 035035
- [14] Wan L, Flegle J, Ozdoganlar B and LeDuc P 2020 Toward vasculature in skeletal muscle-on-a-chip through thermo-responsive sacrificial templates *Micromachines* **11** 907
- [15] Kim W J, Jang C H and Kim G H 2019 A myoblast-laden collagen bioink with fully aligned au nanowires for muscle-tissue regeneration *Nano Lett.* **19** 8612–20
- [16] Mills R J, Parker B L, Monnot P, Needham E J, Vivien C J, Ferguson C, Parton R G, James D E, Porrello E R and Hudson J E 2019 Development of a human skeletal muscle platform with pacing capabilities *Biomaterials* **198** 217–27
- [17] Kim J H, Seol Y-J, Ko I K, Kang H-W, Lee Y K, Yoo J J, Atala A and Lee S J 2018 3D bioprinted human skeletal muscle constructs for muscle function restoration *Sci. Rep.* **8** 12307
- [18] Gholobova D, Gerard M, Decroix L, Desender L, Callewaert N, Annaert P and Thorrez L 2018 Human tissue-engineered skeletal muscle: a novel 3D *in vitro* model for drug disposition and toxicity after intramuscular injection *Sci. Rep.* **8** 1–14
- [19] Afshar M E, Abraha H Y, Bakooshli M A, Davoudi S, Thavandiran N, Tung K, Ahn H, Ginsberg H J, Zandstra P W and Gilbert P M 2020 A 96-well culture platform enables longitudinal analyses of engineered human skeletal muscle microtissue strength *Sci. Rep.* **10** 1–16
- [20] Maffioletti S M *et al* 2018 Three-dimensional human iPSC-derived artificial skeletal muscles model muscular dystrophies and enable multilineage tissue engineering *Cell. Rep.* **23** 899–908
- [21] Somers S M, Zhang N Y, Morrisette-mcalmon J B F, Tran K, Mao H Q and Grayson W L 2019 Myoblast maturity on aligned microfiber bundles at the onset of strain application impacts myogenic outcomes *Acta Biomater.* **94** 232–42
- [22] Christensen R K, Von Halling Laier C, Kiziltay A, Wilson S and Larsen N B 2020 3D printed hydrogel multiassay platforms for robust generation of engineered contractile tissues *Biomacromolecules* **21** 356–65
- [23] Mestre R, Patiño T, Barceló X, Anand S, Pérez-Jiménez A and Sánchez S 2019 Force modulation and adaptability of 3D-bioprinted biological actuators based on skeletal muscle tissue *Adv. Mater. Technol.* **4** 1–13
- [24] Afshar Bakooshli M *et al* 2019 A 3D culture model of innervated human skeletal muscle enables studies of the adult neuromuscular junction *Elife* **8** 1–29
- [25] Madden L, Juhas M, Kraus W E, Truskey G A and Bursac N 2015 Bioengineered human myobundles mimic clinical responses of skeletal muscle to drugs *Elife* **2015** 1–14
- [26] Rao L, Qian Y, Khodabukus A, Ribar T and Bursac N 2018 Engineering human pluripotent stem cells into a functional skeletal muscle tissue *Nat. Commun.* **9** 126
- [27] Khodabukus A, Madden L, Prabhu N K, Koves T R, Jackman C P, Muoio D M and Bursac N 2019 Electrical stimulation increases hypertrophy and metabolic flux in tissue-engineered human skeletal muscle *Biomaterials* **198** 259–69
- [28] Aisenbrey E A and Murphy W L 2020 Synthetic alternatives to Matrigel *Nat. Rev. Mater.* **5** 539–51
- [29] Talbot N C and Caperna T J 2015 Proteome array identification of bioactive soluble proteins/peptides in Matrigel: relevance to stem cell responses *Cytotechnology* **67** 873–83
- [30] Higuchi A, Ling Q-D, Ko Y-A, Chang Y and Umezawa A 2011 Biomaterials for the feeder-free culture of human embryonic stem cells and induced pluripotent stem cells *Chem. Rev.* **111** 3021–35
- [31] Polykandriotis E, Arkudas A, Horch R E, Kneser U and Mitchell G 2008 To matrigel or not to matrigel *Am. J. Pathol.* **172** 1441–2
- [32] Vukicevic S, Kleinman H K, Luyten F P, Roberts A B, Roche N S and Reddi A H 1992 Identification of multiple active growth factors in basement membrane matrigel suggests caution in interpretation of cellular activity related to extracellular matrix components *Exp. Cell Res.* **202** 1–8
- [33] Choi Y-J *et al* 2019 A 3D cell printed muscle construct with tissue-derived bioink for the treatment of volumetric muscle loss *Biomaterials* **206** 160–9
- [34] Kenar H, Ozdogan C Y, Dumlu C, Doger E, Kose G T and Hasirci V 2019 Microfibrous scaffolds from poly(l-lactide-co- $\epsilon$ -caprolactone) blended with xeno-free collagen/hyaluronic acid for improvement of vascularization in tissue engineering applications *Mater. Sci. Eng. C* **97** 31–44
- [35] Parenteau-Bareil R, Gauvin R and Berthod F 2010 Collagen-based biomaterials for tissue engineering applications *Materials* **3** 1863–87
- [36] Khodabukus A and Baar K 2016 Factors that affect tissue-engineered skeletal muscle function and physiology *Cells Tissues Organs* **202** 159–68
- [37] Fekete N *et al* 2012 Platelet lysate from whole blood-derived pooled platelet concentrates and apheresis-derived platelet concentrates for the isolation and expansion of human bone marrow mesenchymal stromal cells: production process,

- content and identification of active com *Cytherapy* **14** 540–54
- [38] Mendes B B, Gómez-Florit M, Babo P S, Domingues R M, Reis R L and Gomes M E 2018 Blood derivatives awaken in regenerative medicine strategies to modulate wound healing *Adv. Drug Deliv. Rev.* **129** 376–93
- [39] Crespo-Diaz R, Behfar A, Butler G W, Padley D J, Sarr M G, Bartunek J, Dietz A B and Terzic A 2011 Platelet lysate consisting of a natural repair proteome supports human mesenchymal stem cell proliferation and chromosomal stability *Cell Transplant.* **20** 797–812
- [40] Fortunato T M, Beltrami C, Emanuelli C, De Bank P A and Pula G 2016 Platelet lysate gel and endothelial progenitors stimulate microvascular network formation *in vitro*: tissue engineering implications *Sci. Rep.* **6** 25326
- [41] Sadeghi-Ataabad M, Mostafavi-Pour Z, Vojdani Z, Sani M, Latifi M and Talei-Khozani T 2017 Fabrication and characterization of platelet-rich plasma scaffolds for tissue engineering applications *Mater. Sci. Eng. C* **71** 372–80
- [42] Mendes B B, Gómez-Florit M, Pires R A, Domingues R M A, Reis R L and Gomes M E 2018 Human-based fibrillar nanocomposite hydrogels as bioinstructive matrices to tune stem cell behavior *Nanoscale* **10** 17388–401
- [43] Mendes B B, Gómez-Florit M, Hamilton A G, Detamore M S, Domingues R M A, Reis R L and Gomes M E 2020 Human platelet lysate-based nanocomposite bioink for bioprinting hierarchical fibrillar structures *Biofabrication* **12** 015012
- [44] Massenet J, Gitiaux C, Magnan M, Cuvellier S, Hubas A, Nusbaum P, Dilworth F J, Desguerre I and Chazaud B 2020 Derivation and characterization of immortalized human muscle satellite cell clones from muscular dystrophy patients and healthy individuals *Acta Biomater.* **9** 1780
- [45] Fernández-Costa J M, Ortega M A, Rodríguez-Comas J, Lopez-Muñoz G, Yeste J, Mangas-Florencio L, Fernández-González M, Martín-Lasierra E, Tejedera-Villafranca A and Ramón-Azcón J 2022 Training-on-a-chip: a multi-organ device to study the effect of muscle exercise on insulin secretion *in vitro* *Adv. Mater. Technol.* **2200873**
- [46] Schindelin J et al 2012 Fiji: an open-source platform for biological-image analysis *Nat. Methods* **9** 676–82
- [47] Schneider C A, Rasband W S and Eliceiri K W 2012 NIH Image to ImageJ: 25 years of image analysis *Nat. Methods* **9** 671–5
- [48] Kalman B, Picart C and Boudou T 2016 Quick and easy microfabrication of T-shaped cantilevers to generate arrays of microtissues *Biomed. Microdevices* **18** 43
- [49] Ramade A, Legant W R, Picart C, Chen C S and Boudou T 2014 Microfabrication of a platform to measure and manipulate the mechanics of engineered microtissues *Methods in Cell Biology* vol 121 (Oxford, UK: Elsevier Inc.) pp 191–211
- [50] Vandenburg H, Shansky J, Benesch-Lee F, Barbata V, Reid J, Thorrez L, Valentini R and Crawford G 2008 Drug-screening platform based on the contractility of tissue-engineered muscle *Muscle Nerve* **37** 438–47
- [51] Iuliano A, van der Wal E, Ruijmbeek C W B, In 't Groen S L M, Pijnappel W W M, PdeGreef J C and Saggiomo V 2020 Coupling 3D printing and novel replica molding for in house fabrication of skeletal muscle tissue engineering devices *Adv. Mater. Technol.* **5** 1–9
- [52] Ebrahimi M et al 2021 De novo revertant fiber formation and therapy testing in a 3D culture model of duchenne muscular dystrophy skeletal muscle *Acta Biomater.* **132** 227–44
- [53] Mendes B B, Gómez-Florit M, Osório H, Vilaça A, Domingues R M A, Reis R L and Gomes M E 2020 Cellulose nanocrystals of variable sulfation degrees can sequester specific platelet lysate-derived biomolecules to modulate stem cell response *Chem. Commun.* **56** 6882–5
- [54] Faralli H and Dilworth F J 2012 Turning on myogenin in muscle: a paradigm for understanding mechanisms of tissue-specific gene expression *Comp. Funct. Genomics* **2012** 836374
- [55] Sanger J W, Chowrashi P, Shaner N C, Spalhoff S, Wang J, Freeman N L and Sanger J M 2002 Myofibrillogenesis in skeletal muscle cells *Clin. Orthop. Relat. Res.* **403** S153–62
- [56] Boudou T, Legant W R, Mu A, Borochin M A, Thavandiran N, Radisic M, Zandstra P W, Epstein J A, Margulies K B and Chen C S 2012 A microfabricated platform to measure and manipulate the mechanics of engineered cardiac microtissues *Tissue Eng. A* **18** 910–9
- [57] Hinds S, Bian W, Dennis R G and Bursac N 2011 The role of extracellular matrix composition in structure and function of bioengineered skeletal muscle *Biomaterials* **32** 3575–83